All-Optical Analog-to-Digital and Digital-to-Analog Conversions Based on Fiber Nonlinearities

Akihiro Maruta and Shoichiro Oda

Graduate School of Engnerring, Osaka University
Osaka 565-0871, Japan
Tel: +81-6-6879-7728; Fax: +81-6-6879-7688; E-mail: maruta@eie.eng.osaka-u.ac.jp

Abstract- **Fiber nonlinearities provide us attractive nonlinear functions for all-optical signal processing. In this paper, we review all-optical analog-to-digital and digital-to-analog conversion schemes based on fiber nonlinearities, including soliton phenomena, Supercontinuum generation, and parametric amplification.**

Index Terms- **Satellite link, signal level, fade slope, rain fade analysis, rain fades modeling.**

I. INTRODUCTION

Recently, the research on all-optical analog-to-digital conversion (ADC) has been extensively attempted to break through inherently limited operating speed of electronic devices [1]. For most of the proposed optical ADC systems, however, the optically sampled pulse sequence is converted to electrical signal. The sampled electrical signal is then quantized by conventional electronic quantizers [2]. Optical quantization and coding are expected to develop for realizing high-speed ADC. While all-optical ADC has been extensively studied, there are only a few works on all-optical digital-to-analog conversion (DAC) [3,4].

In this paper, all-optical ADC and DAC schemes based on fiber nonlinerarities are reviewed. We show numerical and experimental results, which allow us to confirm the feasibility of the schemes.

II. ALL-OPTICAL ADC UTILIZING SOLITON PHENOMENA

2.1 Principle

Figure 1 shows a schematic diagram of the proposed scheme utilizing soliton phenomena [5]. Sampling pulse sequence with central frequency is ω_1 and an analog signal with ω_2, and a continuous wave (CW) with ω_3 are coupled and launched into a zero-dispersion fiber (Fiber 1). A pulse sequence with amplitudes proportional to the sampled analog signal is generated by four-wave mixing (FWM) at $2\omega_1 - \omega_2$. In addition, a constant-amplitude pulse sequence at $2\omega_1 - \omega_3$ is generated. An optical band pass filter (OBPF) selects the pulses at these two frequencies and sends the pulse into a constant anomalous-dispersion fiber (Fiber 2).

The initial value problem of nonlinear Schrödinger equation which governs the evolution of the optical pulse in Fiber 2 can be solved by using the inverse scattering transformation (IST) [6] and its solution consists of a finite number of solitons corresponding to discrete eigenvalues and a dispersive wave corresponding to continuous spectrum. A pulse consisting of a plural number of discrete eigenvalues
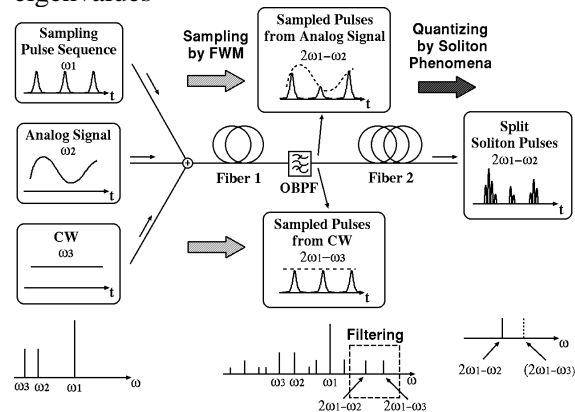

Figure 1 : Schematic diagram of the proposed ADC.

is called a higher-order soliton and the number of discrete eigenvalues varies depending on the amplitude of the sampled pulse. That indicates that the multi-level thresholding process which is indispensable for quantization can be realized in the optical domain. Therefore, in Fiber 2, a pulse sampled from analog signal behaves as a higher-order soliton depending on its own initial amplitude, i.e. a sampled pulse is quantized. In order to count the number of solitons, the higher-order soliton is split into the number of separated solitons due to cross-phase modulation (XPM) induced by a pulse sampled from CW. The quantization scheme based on pulse number modulation (PNM) is feasible.

2.2 Experimental Demonstration

Figure 2 shows the experimental setup for split into solitons. An optical pulse with the pulse width of 2ps and the central wavelength of 1553nm is divided into two pulses by an optical coupler (OC)1. In the upper branch, the pulse is filtered out by an OBPF1 with the central wavelength of 1554nm and amplified by EDFA1 to obtain suitable power for forming a 2nd-order soliton. We here consider the 2nd-order soliton as a sampled pulse. In lower branch, a pulse colliding with the 2nd-order soliton is generated. The pulse is filtered out by an OBPF3 with the central wavelength of 1550nm and amplified by EDFA2. The 2nd-order soliton and the colliding pulse are coupled by an OC2 and the delay line inserted in the lower branch is adjusted to make these pulses overlap completely at the input end of 10km-long non-zero dispersion shifted fiber (NZ-DSF). The averaged input power and the pulse width of the 2nd-order soliton and the colliding pulse are –3dBm, 2.7ps, and –10.7dBm, 2.6ps, respectively. The solid curve in Fig. 3 shows the autocorrelation trace observed at the output of NZ-DSF after the collision. The trace has three peaks, which means that the two separated pulses are observed. The observed pulse spacing between pulses is about 19ps. For comparison, the trace of only 2nd-order soliton without the collision is shown by dotted curve. The trace is different from the solid curve and has only one peak. This result allows us to confirm that the 2nd-order soliton splits into two
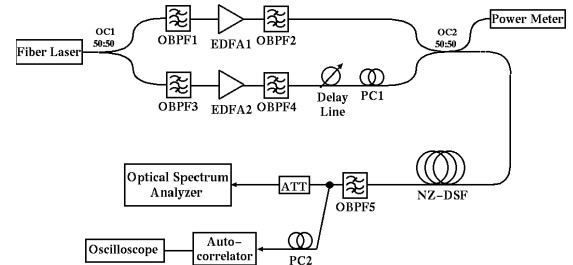

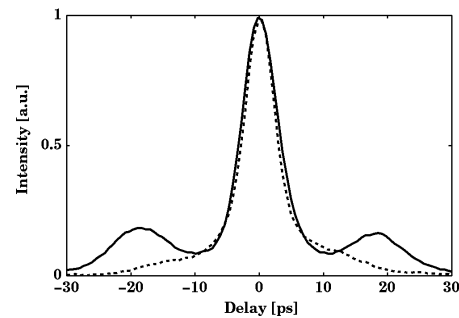Figure 2 : Experimental setup for split into solitons.

Figure 3 : Observed autocorrelation trace at the output of 10km-long NZ-DSF.

separated solitons.

III. ALL-OPTICAL ADC BY SLICING SC SPECTRUM AND SWITCHING WITH NOLM

3.1 Principle

Figure 4 shows the schematic diagram of the proposed 2-bit all-optical ADC scheme by slicing supercontinuum (SC) generation and switching pulses with a nonlinear optical loop mirror (NOLM) [7]. The proposed scheme consists of two stages. In the first stage, a sampled pulse in which the peak power is proportional to the original analog signal is amplified and launched into a normal dispersion-flattened fiber (DFF) for generating SC [8]. The generated SC spectrum is analyzed with an arrayed waveguide grating (AWG) at the output of the DFF. The wavelength allocation of the AWG's output ports is set in the Stokes (or anti-Stokes) side of the central wavelength of the input pulse, as shown in the central bottom of Fig. 4. Since the generated SC spectral width depends on the input peak power launched into the DFF, the number of pulses at the AWG's output ports also depends on

Figure 4 : Schematic diagram of the proposed ADC.

Figure 5: Experimental setup for ADC.

the input peak power of the sampled pulse. This indicates that an optical quantization based on PNM is feasible [9]. In the second stage, an optical coding is performed by switching pulses thanks to XPM in a NOLM. In this scheme, the Gray code for a 2-bit output is used. We assume that the pulses with the wavelength of λ_1 and λ_3 at the AWG's output ports are the signal pulse and the control pulse, respectively. Both of pulses are coupled and launched into a NOLM. Nonlinear phase shift $\Delta\phi_{XPM}$ in the clockwise signal pulse due to XPM is induced by the copropagating control signal. On the other hand, nonlinear phase shift is not induced in the counterclockwise signal pulse, because the counterclockwise control pulse is filtered out by an OBPF at the output of the OC2. While the signal pulse passes through the NOLM and is absorbed in the terminator for $\Delta\phi_{XPM} = \pi$, the pulse is reflected by the NOLM and passes through the circulator to the output port for $\Delta\phi_{XPM} = 0$. The reflected signal pulse with the wavelength of λ_1 for $\Delta\phi_{XPM} = 0$ and the pulse with λ_2 at the AWG's output port are assigned to the least significant bit (LSB) and the most significant bit (MSB), respectively. For the analog signal of "0", no pulse appears at the output ports. Therefore, the coded digital signal is "00". For the analog signal of "1", only signal pulse with λ_1 is launched into the NOLM. The signal pulse is reflected by the NOLM because $\Delta\phi_{XPM} = 0$. We then obtain the digital signal "01". For the analog signal of "2", an additional pulse with λ_2 is obtained at the output port. The

(a) OBPF1

(b) NOLM

Figure 6: Transfer function measured at the output of the OBPF1 and the NOLM.

digital signal is then "11". Finally, for the analog signal of "3", both of the control pulse with λ_3 and the signal pulse are launched into the NOLM. By appropriately designing the NOLM so that $\Delta\phi_{XPM} = \pi$, the signal pulse then passes through the NOLM and is absorbed in the terminator. Therefore, the digital signal is "10". Consequently, the quantized signal based on PNM can be assigned to the digital signal using the Gray code.

3.2 Experimental Demonstration

The experimental setup for 2-bit all-optical ADC is shown in Fig. 5. Optical pulses with the pulse width of 2ps and the central wavelength of 1561nm are launched into a DFF to generate SC. The group velocity dispersion, the dispersion slope, the nonlinear coefficient, and the length of the DFF are -1.93ps/nm/km, -0.001ps/nm^2/km, 3.9W^{-1}/km and 1.5km, respectively. The generated SC spectrum is filtered out at 1556nm by an OBPF1 as a virtual output port of an AWG. The filled circles and the solid line in Fig. 6(a) show the transfer function measured at the output of the OBPF1 and the corresponding binary output as functions of the input peak power to DFF, respectively. As one notices, the binary output represents the MSB of the 2-bit Gray code.

Next, the generated SC is divided by an OC1. In the upper branch, the SC spectrum is filtered out by an OBPF2 with the bandwidth of 1nm and the central wavelength of 1559nm. We assign the obtained pulseto the signal pulse. In the lower branch, the SC spectrum is filtered out by an OBPF4 with the bandwidth of 0.5nm and central wavelength of 1553nm. The obtained pulse is assigned to the control pulse. After both of pulses are amplified by EDFAs2 and 3, the pulses launched into the NOLM consisting of DSF in which the zero dispersion wavelength, the dispersion slope, the nonlinear coefficient, and the length of the DSF are 1556nm, 0.06ps/nm^2/km, 2.1W^{-1}/km, and 5km, respectively. The filled circles in Fig. 6(b) shows the transfer function of signal pulse at the output of the NOLM with varying the input
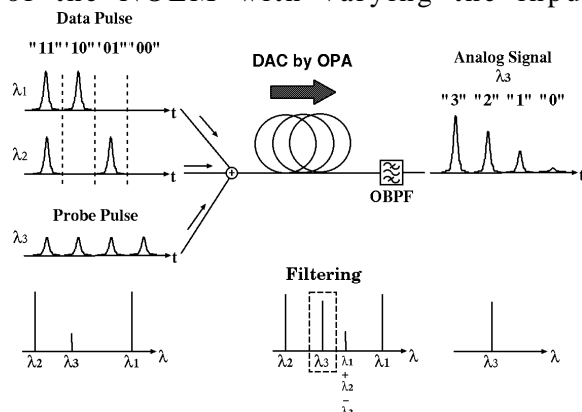

Figure 7: Schematic diagram of the proposed DAC.

average power of the signal pulse and the control pulse. The binary output is illustrated by the solid line in Fig. 6(b). As can be seen, the binary output represents the LSB. We have successfully demonstrated the qualitative feasibility of the proposed 2-bit all-optical ADC.

IV. ALL-OPTICAL DAC UTILIZING OPA
4.1 Principle

Figure 7 shows the schematic diagram of the proposed DAC scheme [10]. The parallelized 2-bit optical data pulses with which the central wavelength of each bit is λ_1 and λ_2, and the peak power of that is P_{p1} and P_{p2}, are used as pump lights for OPA. Amplified data pulses and a probe pulse with λ_3 are coupled and launched into a fiber as a parametric gain medium. In the fiber, the probe pulse is amplified due to parametric process and its gain G [dB] is given by [11]

$$G = 10\log_{10}\left\{1 + \left(\frac{\gamma P}{g}\right)^2 \sinh^2(gL)\right\}, \quad (1)$$

where γ and L is the nonlinear coefficient and the fiber length, respectively. The parametric gain coefficient g is expressed as $g = \sqrt{(\gamma P)^2 - \left(\kappa/2\right)^2}$. In the case of dual pump OPA which corresponds to the digital signal "11", the total pump power P and the total phase mismatch κ are given by $P = 2\sqrt{P_{p1}P_{p2}}$,
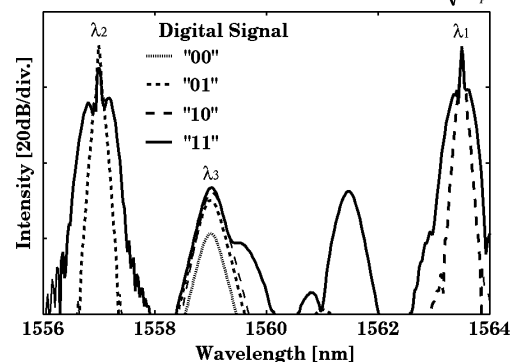

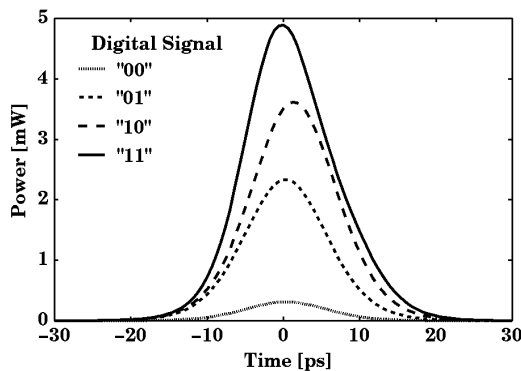Figure 8: Numerically obtained spectra at the output of DSF.

Figure 9: Numerically obtained temporal waveforms after filtering.

$\kappa = \Delta\beta + \gamma(P_{p1} + P_{p2})$, where $\Delta\beta$ is linear phase mismatch. In the case single pump OPA which corresponds to "01" or "10", $P = P_{pn}$, $\kappa = \Delta\beta + 2\gamma P_{pn}$ $(n = 1,2)$. Equation (1) shows that the parametric gain G depends on P and κ. Therefore we can convert the digital signal, "01", "10" , and "11" to the analog signal "1", "2", and "3" by appropriately setting the pump wavelengths λ_1 , λ_2 and powers P_{p1} , P_{p2}. Note that, in the case of "00", we can consider the weak probe pulse as "0". After filtering out the amplified pulse by an OBPF to remove the pump lights and the redundant idler lights, we can obtain the analog signal. The proposed DAC scheme can be used to OOK-to-Quaternary ASK modulation format converter, in which the parallelized OOK date are converted to the serial Quaternary ASK data.

4.2 Numerical Simulation

We conducted numerical simulation to confirm the feasibility of the proposed DAC scheme. The zero dispersion wavelength, the dispersion slope, the nonlinear coefficient, and the length of the DSF used in the simulation are 1556nm, 0.03ps/nm^2/km, 2.1W^{-1}/km, and 2.4km, respectively. A hyperbolic-secant shape pulse with the pulse width (FWHM) of 10ps, the peak power of 0.5mW, and the central wavelength of 1559nm is used as a probe pulse. The pump pulses have a super-Gaussian shape with the pulse width of 100ps to neglect the walk-off between the probe and the pump pulses. Their central wavelengths, λ_1 and λ_2 , are set to

1563.5nm and 1557nm, respectively. We set λ_1 and λ_2 in the wavelength range with having exponential gain. The pump power P_{p1} , P_{p2} is 0.5W $(P_{p1} = P_{p2})$. The filter has Gaussian-shape and its bandwidth is 0.4nm. The spectra obtained at the output of the DSF are shown by several kinds of dotted lines and the solid line in Fig. 8. The probe pulse is amplified due to parametric process depending on the digital signal, "01"-"11". In the case of "00", the probe pulse is not amplified. Figure 9 shows the temporal waveforms after filtering by the OBPF. One can see that the output peak power varies depending on the digital signals, which means that the digital signals can be converted to analog signals by OPA. Although numerically obtained signal level is not ideally "0"-"3", the level can be flexibly controlled by changing the pump power, the wavelength allocation of the pump and probe pulses, and the fiber parameters.

V. CONCLUSION

In this paper, we have reviewed two all-optical ADC schemes and an all-optical DAC scheme. A higher-order soliton formation and SC generation depending on the peak power are applied to multi-level thresholding process in the optical domain. OPA in fiber realizes an optical summation which is indispensable process for DAC without controlling the phase of pulses. Since all schemes can be performed by using only fiber nonlinearities without any electronic devices, they can operate beyond 40GHz.

REFERENCES

[1] B. L. Shoop, "Photonic analog-to-digital conversion," (Springer, Berlin, 2001).
[2] J. C. Twichell *et al., IEEE Photon. Technol. Lett.,* **12**, 236-238, 2000.
[3] T. Saida *et al., Electron. Lett.,* **37**, 1237-1238, 2001.
[4] A. Yacoubian *et al., IEEE Photon. Technol. Lett.*, **15**, 117-119, 2003.
[5] S. Oda, A. Maruta, and K. Kitayama, *IEEE Photon. Technol. Lett.,* **16**, 587-589, 2004.
[6] V. E. Zakharov and A. B. Shabat, Sov. Phys. JETP, **34**, 62-69, 1972.
[7] S. Oda and A. Maruta, *in Proc. OFC 2005,* Paper OThN3, California, USA, 2005.

[8] Y. Takushima *et al., IEEE Photon. Technol. Lett.*, **10**, 1560-1562, 1998.

[9] S. Oda and A. Maruta, *IEEE Photon. Technol. Lett.,* **17**, 465-467, 2005.

[10] S. Oda and A. Maruta, *in Proc. CPT 2005,* Paper P-7, Tokyo, Japan, 2005.

[11] R. H. Stolen *et al., IEEE J. Quantum Electron.,* QE-18, 1062-1071, 1982.

Fated as shown in Fig. 1. In these stations, we observe the received signal level (every 0.2 second).